



# The Glycogen Synthase Kinase–3 Inhibitor CHIR99021 Reduces Fatty Infiltration and Muscle Atrophy After Rotator Cuff Tears

## An In Vitro Experiment and In Vivo Mouse Model

Pu Zhang,<sup>\*</sup> MD , Meng Zhou,<sup>†‡</sup> MD, Yiming Zhu,<sup>†</sup> MD, Jianhao Xie,<sup>\*</sup> MD , Ziqi Huo,<sup>†</sup> MD, Dan Zhang,<sup>\*</sup> MD, Pinxue Li,<sup>\*</sup> MD, Jianxun Guo,<sup>§</sup> Guangping Li,<sup>‡</sup> Xu Li,<sup>†</sup> MD, Renxian Wang,<sup>§||</sup> PhD, and Chunyan Jiang,<sup>\*†‡||</sup> MD, PhD

*Investigation performed at Sports Medicine Service, Beijing Jishuitan Hospital, Capital Medical University, Beijing, China*

**Background:** Rotator cuff tears (RCTs) can cause inflammation, muscle atrophy, and irreversible fatty infiltration, resulting in poor clinical outcomes. Effective therapeutic approaches to inhibit fatty infiltration in rotator cuff muscles remain limited.

**Purpose:** To identify pathways associated with fatty infiltration through RNA sequencing and to evaluate the therapeutic potential of the glycogen synthase kinase–3 (GSK-3) inhibitor CHIR99021 based on enrichment of the Akt/GSK-3 pathway identified by RNA sequencing.

**Study Design:** Controlled laboratory study.

**Methods:** Supraspinatus muscle biopsy specimens from 6 patients with chronic full-thickness RCTs were analyzed by RNA sequencing. Fibro-adipogenic progenitors (FAPs) or C2C12 myoblasts were cultured with different doses of CHIR99021 to assess their effects on adipogenic or myogenic differentiation, respectively. RNA sequencing identified cellular pathways in FAPs treated with or without CHIR99021. A mouse RCT model was established by detaching the supraspinatus tendon, followed by treatment with or without CHIR99021 administered intraperitoneally. Muscle atrophy and fatty infiltration were assessed histologically and through gene expression analysis at 1 and 4 weeks after surgery.

**Results:** RNA sequencing analysis identified a marked upregulation of the Akt/GSK-3 signaling pathway specifically in patients' samples and FAPs with minimal fat accumulation. CHIR99021 suppressed adipogenic differentiation in FAPs and promoted myogenic differentiation in C2C12 cells. In the mouse RCT model, CHIR99021-treated mice exhibited reduced Oil Red O staining, a larger cross-sectional area, and less muscle weight loss in the supraspinatus muscle compared with the vehicle-treated mice. Gene expression analysis indicated increased myogenesis and reduced fatty infiltration at 1 and 4 weeks after surgery as well as increased expression levels of IL-6 and IL-15 in the CHIR99021 group compared with the control group at 1 week after surgery.

**Conclusion:** The Akt/GSK-3 pathway was enriched in supraspinatus muscle samples and FAPs with low fat accumulation, highlighting its potential as a therapeutic target. The GSK-3 inhibitor CHIR99021 was shown to alleviate fatty infiltration and muscle atrophy after RCTs in vitro and in vivo in a mouse model.

**Clinical Relevance:** The GSK-3 inhibitor CHIR99021 shows potential for treating muscle degeneration after RCTs.

**Keywords:** rotator cuff tears; fatty infiltration; muscle atrophy; fibro-adipogenic progenitors; glycogen synthase kinase–3

A rotator cuff tear (RCT) is one of the most common shoulder injuries, resulting in muscle degeneration in patients.<sup>19</sup> Muscle degeneration, which includes muscle atrophy and fatty infiltration, is correlated with high

retear rates and poor clinical outcomes after rotator cuff repair.<sup>9,14,37</sup> Fatty infiltration, a major contributor to poor muscle quality, is associated with various factors such as age, tear size, traumatic injuries, tendon retraction, and suprascapular neuropathy.<sup>6,15,17,27</sup> Furthermore, fatty infiltration is considered irreversible and progressive, even after complete restoration of the rotator cuff.<sup>8,18</sup> Despite numerous studies providing valuable insights,<sup>11,32,38</sup> the cellular and molecular processes underlying fatty infiltration in rotator cuff muscles remain



largely unknown. Therefore, understanding these mechanisms and developing effective therapies for fatty infiltration are crucial for improving clinical outcomes in patients with rotator cuff degeneration.

Muscle tissue harbors a resident population of PDGFR $\alpha$ -positive stem cells known as fibro-adipogenic progenitors (FAPs), which process the ability to differentiate into fibroblasts and adipocytes, leading to ectopic fat accumulation.<sup>12,35</sup> The pathophysiological roles of FAPs in tissue exhibit both beneficial and detrimental aspects. In the context of minor or repairable injuries, FAPs contribute to muscle homeostasis and regeneration.<sup>7</sup> However, under pathological conditions, FAPs proliferate and differentiate into adipocytes and myofibroblasts, contributing to tissue damage.<sup>24</sup> Previous research has demonstrated that FAPs are primarily regulated by several pathways, including ciliary pathways,<sup>16</sup> retinoic acid signaling,<sup>39</sup> nitric oxide,<sup>3</sup> TGF- $\beta$ ,<sup>24</sup> and activin-dependent signaling pathways.<sup>23</sup> Additionally, the inflammatory process exerts a complex influence on both adipogenesis and myogenesis. Cytokines such as IL-4, IL-6, IL-13, and IL-15 modulate the proliferation of FAPs or their capacity to regulate muscle mass and degeneration.<sup>10,13,29</sup> In addition, studies have shown that certain pharmacological agents, such as TGF- $\beta$  inhibitors,<sup>4</sup> retinoic acid receptor agonists,<sup>32</sup> parathyroid hormone,<sup>11</sup> and metformin,<sup>40</sup> can suppress the adipogenic differentiation of FAPs or mitigate fatty infiltration in animal models of RCTs. However, there are currently no effective pharmaceutical interventions for rotator cuff degeneration in patients, emphasizing the need for new mechanistic understanding and the development of targeted therapeutics. RNA sequencing analysis of human samples has highlighted the distinct enrichment of the Akt and Wnt pathways, correlating with varying levels of fatty infiltration. Studies have shown that the Akt/glycogen synthase kinase-3 (GSK-3)/ $\beta$ -catenin<sup>25</sup> and WNT5a/GSK-3/ $\beta$ -catenin<sup>31</sup> pathways regulate the differentiation of FAPs. The activation of WNT5a and Akt enhances GSK-3/ $\beta$ -catenin signaling, suppressing PPAR- $\gamma$  expression and thus inhibiting the adipogenesis of FAPs. Given the role of GSK-3 as a critical negative regulator in the Wnt/ $\beta$ -catenin pathway, the pharmacological inhibition of GSK-3 has been shown to stabilize  $\beta$ -catenin, reduce PPAR- $\gamma$  levels, and ultimately prevent the adipogenic differentiation of FAPs.<sup>31</sup> This evidence positions GSK-3/ $\beta$ -

catenin signaling as a promising target for controlling FAP-mediated fatty infiltration, which is a hallmark of RCTs. However, the effects of GSK-3 inhibitors on RCTs remain unexplored, prompting our focus on investigating the effect of the GSK-3 inhibitor CHIR99021 in this study. We selected CHIR99021 as a representative GSK-3 inhibitor because of its high activity and low toxicity among 4 different GSK-3 inhibitors.<sup>30</sup>

In this study, RNA sequencing was employed to elucidate the underlying mechanisms of fatty infiltration in patients' rotator cuff muscles. On the basis of RNA sequencing analysis, we selected CHIR99021, a potent GSK-3 inhibitor, to assess its therapeutic efficacy in a mouse model of RCTs. We hypothesized that supraspinatus muscle samples with lower degrees of fatty infiltration, as determined by magnetic resonance imaging (MRI), would exhibit a pronounced activation of the Akt/GSK-3 pathway and that the GSK-3 inhibitor CHIR99021 could effectively suppress fat accumulation and muscle atrophy both in vitro and in a mouse model of RCTs.

## METHODS

### Isolation of FAPs From Mouse Muscle

Male C57BL/6J mice were sacrificed, and their hindlimb muscles were dissected and minced. Muscle tissue was digested with 0.2% collagenase type II (Thermo Fisher Scientific) for 90 minutes, followed by 0.4% dispase (Thermo Fisher Scientific) for 30 minutes at 37°C, and then filtered through 100- and 70- $\mu$ m cell strainers (Corning). For fluorescence-activated cell sorting, the cell suspension was stained with APC-PDGFR $\alpha$  (Cat #135908; BioLegend), PE-CD31 (Cat #160204; BioLegend), PITC-CD45 (Cat #157214; BioLegend), and PE-cyanine 7–Sca-1 (Cat #108114; BioLegend) for 30 minutes at 4°C. PDGFR $\alpha$ -positive/Sca-1–positive/CD31-negative/CD45-negative murine FAPs were isolated using a FACS Aria III cell sorter (BD Biosciences) as previously described.<sup>34</sup>

### Cell Culture, Adipogenic Differentiation, and Treatment

The isolated FAPs were plated on Matrigel (Corning)–coated 12-well plates and cultured in growth medium

<sup>||</sup>Address correspondence to Renxian Wang, PhD, JST Sarcopenia Research Centre, Beijing Research Institute of Traumatology and Orthopaedics, Beijing Jishuitan Hospital, Capital Medical University, No. 31 Xijiekoudongjie, Xicheng District, Beijing, 100035, China (email: wrxpumc@126.com); and Chunyan Jiang, MD, PhD, Sports Medicine Service, Beijing Jishuitan Hospital, Capital Medical University, No. 31 Xijiekoudongjie, Xicheng District, Beijing, 100035, China (email: chunyanj@hotmail.com).

\*Fourth School of Clinical Medicine, Peking University, Beijing, China.

<sup>†</sup>Sports Medicine Service, Beijing Jishuitan Hospital, Capital Medical University, Beijing, China.

<sup>‡</sup>Beijing Research Institute of Traumatology and Orthopaedics, Beijing Jishuitan Hospital, Capital Medical University, Beijing, China.

<sup>§</sup>JST Sarcopenia Research Centre, Beijing Research Institute of Traumatology and Orthopaedics, Beijing Jishuitan Hospital, Capital Medical University, Beijing, China.

P.Z. and M.Z. contributed equally to this article.

Submitted July 12, 2024; accepted December 10, 2024.

One or more of the authors has declared the following potential conflict of interest or source of funding: Funding was received from the National Natural Science Foundation of China (82172513), Natural Science Foundation of Beijing (7244358), Beijing Municipal Public Welfare Development and Reform Pilot Project for Medical Research Institutes (JYY2023-11), and Beijing Municipal Health Commission (BJRITO-RDP-2024). AOSM checks author disclosures against the Open Payments Database (OPD). AOSM has not conducted an independent investigation on the OPD and disclaims any liability or responsibility relating thereto.

(GM), consisting of high-glucose Dulbecco's modified Eagle medium supplemented with 20% fetal bovine serum and 1% penicillin/streptomycin. For adipogenic differentiation, FAPs were cultured in adipogenic induction medium (AIM), containing GM supplemented with 1  $\mu$ g/mL insulin, 1  $\mu$ M dexamethasone, and 0.5 mM 3-isobutyl-1-methylxanthine, for 3 days. Specifically, for Oil Red O staining, the cells underwent an additional 3-day culture period in adipocyte maintenance medium, which included GM supplemented with 1  $\mu$ g/mL insulin. CHIR99021 was reconstituted in dimethyl sulfoxide (DMSO) as directed by the manufacturer. For pharmacological therapy, the CHIR99021 solution or the same volume of DMSO was added to GM or AIM for further experiments. C2C12 myoblasts were grown in high-glucose Dulbecco's modified Eagle medium supplemented with 10% fetal bovine serum and 1% penicillin/streptomycin for 5 days, with or without CHIR99021.

#### Reverse Transcription–Quantitative Polymerase Chain Reaction (RT-qPCR) Analysis

FAPs were cultured in GM, AIM, or AIM containing 3  $\mu$ M CHIR99021 for 3 days to evaluate the expression of PPAR- $\gamma$ , FABP4, CEBPA, and GSK-3. C2C12 cells were treated with 3  $\mu$ M CHIR99021 or the same volume of DMSO to assess the myogenic potential by evaluating the expression of myogenin, Myf5, and desmin. The supraspinatus muscles of mice treated with CHIR99021 or a vehicle were evaluated for the expression of PPAR- $\gamma$ ,  $\beta$ -catenin, myogenin, Myf5, IL-6, and IL-15. Total RNA was extracted using TRIzol reagent (Invitrogen) and converted to complementary DNA with the PrimeScript 1st Strand cDNA Synthesis Kit (6110A; Takara). RT-qPCR was performed using LightCycler 480 Instrument II (Roche) with a real-time qPCR kit (TB Green Premix Ex Taq II [RR420A]; Takara).

#### Western Blot Analysis

FAPs and C2C12 cells were lysed using ice-cold radioimmunoprecipitation assay buffer to extract total proteins. Protein concentrations were measured using the BCA Protein Assay Kit (Cell Signaling Technology). Equal amounts of protein were transferred to a polyvinylidene difluoride membrane. The polyvinylidene difluoride membranes were blocked in skimmed milk at room temperature for 1 hour. Primary antibodies were incubated overnight at 4°C as follows: anti- $\beta$ -tubulin (Solarbio), anti-myosin heavy chain (B-5; Santa Cruz Biotechnology), and anti-non-phosphorylated (active)  $\beta$ -catenin (Cell Signaling Technology). Subsequently, the membranes were incubated with horseradish peroxidase-conjugated secondary antibodies for 1 hour at room temperature. Protein bands were visualized using an enhanced chemiluminescence kit (Millipore), with  $\beta$ -tubulin serving as the control.

#### Animals and Surgical Procedures

Male 8-week-old C57BL/6J mice were housed in a specific pathogen-free environment with a 24-hour light-dark cycle

and ad libitum access to food and water. A total of 40 mice were randomly divided into 2 groups (vehicle vs CHIR99021 treatment;  $n = 20/\text{group}$ ) and underwent complete supraspinatus tendon detachment in the left shoulder after being anesthetized by ketamine and dexmedetomidine via injections to the hip muscles. The randomization process was conducted by an author (J.X.) to ensure blinding. The surgical procedures were performed as previously described.<sup>22</sup> Briefly, a lateral skin incision was made on the left shoulder to expose and cut the supraspinatus tendon completely from the greater tuberosity, partially detaching the muscle from the scapular fossa. The skin was then sutured without repairing the tendon. The right shoulder served as the control. Starting from 3 days after surgery, a vehicle (5% DMSO, 40% PEG 300, 5% Tween 80, and 50% normal saline) or CHIR99021 (15 mg/kg; Selleck Chemicals) was intraperitoneally injected every day. Mice were sacrificed at 1 or 4 weeks after surgery. Bilateral supraspinatus muscles were harvested and weighed. Muscle wet weight loss was calculated using the following formula as previously reported<sup>36</sup>:  $(SS_{\text{Left}} - SS_{\text{Right}})/SS_{\text{Right}} \times 100\%$ . Harvested tissue was used for RT-qPCR ( $n = 5/\text{group}$ ) and tissue section staining ( $n = 5/\text{group}$ ). The Animal Ethics Committee of our hospital approved the animal experiments.

#### Oil Red O Staining

Tissue sections of the supraspinatus muscle and FAPs were fixed in 4% paraformaldehyde for 30 minutes at room temperature. Then, 0.3% Oil Red O stock solution (Cat #O0625; Sigma-Aldrich) in 2-propanol was diluted 3:2 (Oil Red O:ddH<sub>2</sub>O) and passed through a 0.22- $\mu$ m syringe filter. The fixed sections and cells were stained with Oil Red O solution for 10 minutes. The samples were washed 3 times with phosphate-buffered saline (PBS) and underwent imaging using fluorescence microscopy. Lipid droplets stained with Oil Red O underwent excitation using green light, resulting in red fluorescence emission. To quantitatively assess the degree of adipose accumulation, the percentage of FAPs and the area of the supraspinatus sections positively stained with Oil Red O were calculated using ImageJ software (National Institutes of Health).

#### Immunohistochemistry

FAPs were fixed in 4% paraformaldehyde for 30 minutes, washed 3 times in PBS, and permeabilized with 0.1% Triton X-100 (Solarbio) in PBS for 15 minutes. The blocking solution consisted of 5% goat serum and 0.3% Triton X-100 in PBS. For  $\alpha$ -SMA (1:500; Cat #14-9760-82 [Invitrogen]) staining, samples were incubated in the blocking solution for 1 hour and then in primary antibodies diluted in PBS overnight at 4°C. The samples were washed 3 times in PBST (0.05% Tween 20 in PBS) and incubated in diluted secondary antibodies (1:2000; Cat #A11001 [Invitrogen]) for 40 minutes in the dark. After washing the samples 3 times in PBST, they were incubated in diluted DAPI



(1:400; Cat #D9542 [Sigma-Aldrich]) for 10 minutes, followed by another 3 washes. Images were recorded using an inverted microscope (DMI8; Leica). Tissue sections of the supraspinatus were fixed in 4% paraformaldehyde for 1 day and embedded in paraffin. Sections were incubated with anti-perilipin (1:100; Cat #3470 [Cell Signaling Technology]), anti-laminin (1:50; Cat #L9393 [Sigma-Aldrich]), and PDGFR $\alpha$  (1:500; Cat #3174s [Cell Signaling Technology]), followed by the same steps as described above. The images were analyzed using ImageJ software.

### Patient Selection and Biopsy

Patient selection and biopsy obtainment were approved by the institutional review board of our hospital. Patients were recruited from our hospital between August 2022 and April 2023. Inclusion criteria were patients with a chronic full-thickness tear of the supraspinatus tendon diagnosed by MRI before surgery. All patients provided consent to our institute. During arthroscopic surgery, biopsy specimens ( $\sim 3 \times 3$  mm in size) of the supraspinatus muscle were obtained 2 to 3 cm from the muscle-tendon junction as previously described.<sup>5</sup> The degree of fatty infiltration in the supraspinatus muscle was assessed using the Goutallier staging system on MRI. Overall, 3 specimens exhibiting the highest degree of fatty infiltration and 3 specimens with the lowest degree were selected for RNA sequencing analysis.

### RNA Sequencing

The isolated FAPs were cultured in GM, AIM, or AIM containing 3  $\mu$ M CHIR99021 for 3 days. Additionally, specimens from 3 patients with the highest degree of fatty infiltration and 3 patients with the lowest degree were selected. Total RNA was isolated using the RNeasy Pure Tissue Kit (DP431; Qiagen). RNA quality and concentration were assessed using the RNA 6000 Nano Kit (Agilent Technologies). Barcoded RNA libraries were constructed using the VAHTS Universal V6 RNA-seq Library Prep Kit for Illumina (NR604-01/02; Vazyme) according to the manufacturer's instructions. RNA sequencing was performed with the NovaSeq 6000 S4 Sequencing System (Illumina). For differential gene expression analysis between groups, genes with  $|\log_2 \text{ratio}| \geq 1$  and  $q < 0.05$  were considered differentially expressed. DESeq2 software (Version 1.6.3) was used to identify the number of upregulated and downregulated genes. KEGG (Kyoto Encyclopedia of Genes and Genomes) pathway enrichment analysis (<http://www.genome.jp/kegg/>) was conducted using a hypergeometric test to identify significantly enriched pathways among the differentially expressed genes (DEGs).

### Statistical Analysis

Statistical analyses were performed using Prism (Version 9; GraphPad Software) and SPSS (Version 26.0; IBM). Experimental findings are presented as mean  $\pm$  standard

deviation. Differences between the 2 groups were assessed using the Student *t* test, while multiple comparisons were evaluated using 1-way analysis of variance. A *P* value  $< .05$  was considered statistically significant. Each experiment was replicated at least 3 times, yielding consistent results.

## RESULTS

### Predominant Enrichment of Akt/GSK-3 Pathway in Samples Classified as Goutallier Stage 0 Fatty Infiltration

We analyzed patients' samples classified as Goutallier stage 0 and stage 2 on presurgical MRI, with 3 samples per group (Figure 1A). We first identified DEGs between the 2 groups and visualized the results using volcano plots to show the number of upregulated and downregulated genes (Figure 1B). Notably, the samples classified as stage 2 showed a significantly elevated expression of adipogenesis-related genes, consistent with the MRI findings (Figure 1C).

Pathway enrichment analysis of DEGs indicated significant involvement of the PPAR, PI3K-Akt, and Wnt signaling pathways. The PI3K-Akt pathway had the most enriched genes, suggesting its critical role in fatty infiltration (Figure 1D). The PI3K-Akt and Wnt pathways converge on the GSK-3/ $\beta$ -catenin axis, which regulates PPAR- $\gamma$  expression.<sup>25</sup> Therefore, we analyzed the gene expression levels in the Akt/GSK-3 pathway between the 2 groups with a heatmap. Heatmap analysis showed that stage 2 samples had a lower gene expression in the PI3K-Akt pathway and higher GSK-3–related gene expression compared with stage 0 samples (Figure 1E). These findings suggest that suppression of the Akt/GSK-3 pathway may contribute to the accumulation of adipose tissue in the supraspinatus muscle. Thus, targeting the Akt/GSK-3 pathway could be a promising therapeutic approach for treating RCTs.

### CHIR99021 Suppresses Adipogenesis of FAPs and Promotes Myogenesis in C2C12 Cells In Vitro

To assess whether the GSK-3 inhibitor CHIR99021 can mitigate muscle degeneration in vitro, we applied CHIR99021 to FAPs and C2C12 cells to evaluate its effect on adipogenesis and myogenesis. FAPs sorted by fluorescence-activated cell sorting were treated with CHIR99021 at concentrations ranging from 100 nM to 50  $\mu$ M. Oil Red O staining revealed a dose-dependent decrease in the adipocyte percentage, with significant reductions at  $\geq 3$   $\mu$ M ( $P < .001$ ) (Figure 2, A and B). Cell viability demonstrated that concentrations of  $\geq 10$   $\mu$ M negatively impacted FAP viability ( $P < .001$ ) (Figure 2C), identifying 3  $\mu$ M as the optimal concentration for inhibiting adipogenesis without cytotoxicity.

CHIR99021 significantly reduced the gene expression levels of adipogenic markers such as PPAR- $\gamma$ , FABP4, and CEBPA ( $P < .001$ ) (Figure 2D). Adipogenic induction



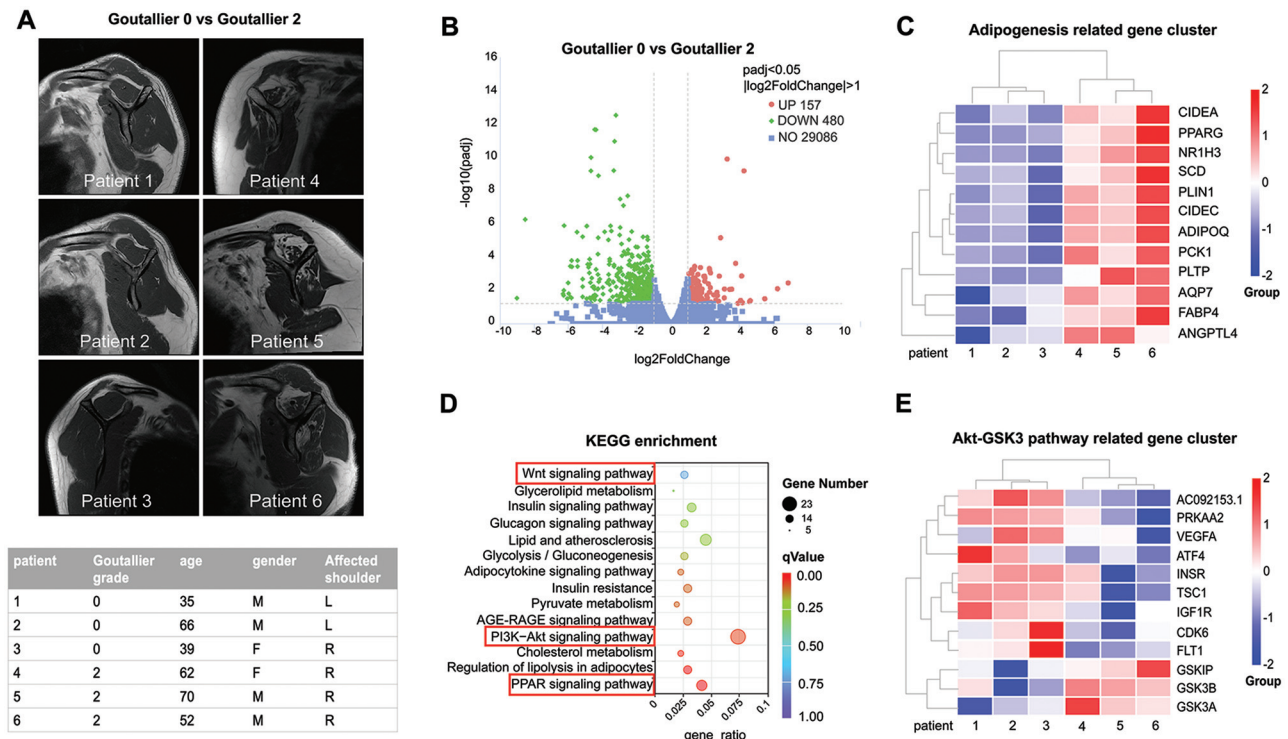


**Figure 1.** RNA sequencing analysis of supraspinatus muscle samples from the rotator cuff. (A) Magnetic resonance imaging and demographic characteristics of 6 patients with rotator cuff tears, grouped by Goutallier stage. n = 3 per group. (B) Volcano plot showing differentially expressed genes (DEGs) between Goutallier stage 0 and stage 2 groups. (C) Clustering heatmap of adipogenesis-related gene expression levels. (D) KEGG (Kyoto Encyclopedia of Genes and Genomes) pathway enrichment analysis of DEGs between the 2 groups. (E) Heatmap of gene expression levels in the Akt/GSK-3 pathway.

increased GSK-3 expression, which was countered by CHIR99021, suggesting that GSK-3 activation contributes to adipogenesis ( $P < .001$ ) (Figure 2D). Western blot analysis showed elevated levels of  $\beta$ -catenin and phosphorylated GSK-3 $\beta$  (Ser9; ie, inactive GSK-3) in FAPs cultured in GM. These levels decreased upon adipogenic induction but were restored with CHIR99021 treatment (Figure 2E).

In C2C12 cells treated with 3  $\mu$ M CHIR99021, myogenic markers such as myogenin, Myf5, and desmin were significantly upregulated compared with the control group ( $P < .01$ ) (Figure 3A). In addition, the myosin heavy chain level was increased with CHIR99021 treatment, as shown by western blotting (Figure 3B). Collectively, our results demonstrated that CHIR99021 suppressed the adipogenic differentiation of FAPs by downregulation of the GSK-3/ $\beta$ -catenin axis and concurrently promoted myogenesis in C2C12 cells.

### Transcriptomic Profiling Reveals That CHIR99021 Regulates Adipogenesis of FAPs by Akt Signaling Pathway

To understand the underlying mechanisms of CHIR99021 in controlling the adipogenic fate of FAPs, RNA sequencing was performed on FAPs cultured in GM, AIM, and AIM with CHIR99021. Principal component analysis showed

distinct gene expression profiles among the conditions (Figure 4A). A clustering heatmap confirmed that CHIR99021 suppressed the adipogenic differentiation of FAPs (Figure 4B). Pathway enrichment analysis of DEGs revealed that the PI3K-Akt, PPAR, and Wnt signaling pathways played crucial roles in adipogenic differentiation (Figure 4C). Specifically, the PI3K-Akt and Wnt signaling pathways were downregulated in AIM compared with GM but were upregulated by CHIR99021 treatment (Figure 4, C and D). Conversely, the PPAR pathway was upregulated in AIM compared with GM and downregulated by CHIR99021. These results suggest that the PI3K-Akt pathway is fundamentally crucial for adipogenesis and that CHIR99021 modulates adipogenesis through this pathway, indicating its potential as a therapeutic target.

### CHIR99021 Suppresses Fatty Infiltration and Muscle Atrophy in Mice

We established an RCT model in mice by detaching the supraspinatus tendon from the humeral head to investigate the potential of CHIR99021 in mitigating fatty infiltration and muscle atrophy. The experimental timeline is illustrated in a schematic diagram (Figure 5A). Mice with RCTs received daily intraperitoneal injections of 15 mg/kg CHIR99021 starting from 3 days after surgery. No

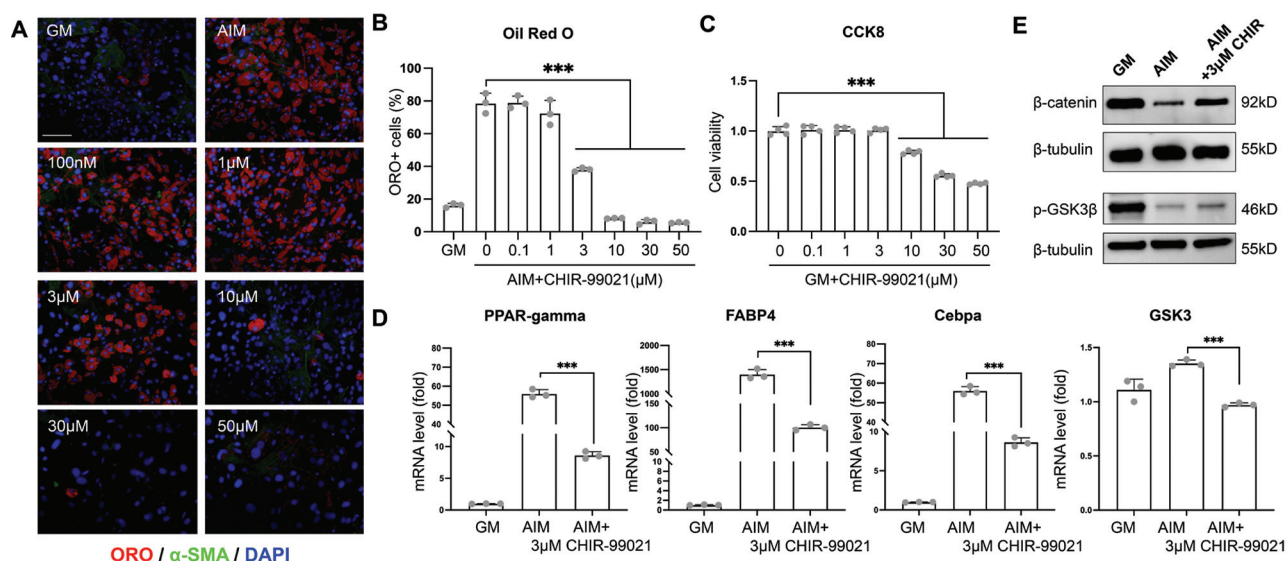


**Figure 2.** Effect of CHIR99021 on the differentiation, viability, and gene expression of fibro-adipogenic progenitors (FAPs) in adipogenic conditions. (A) Immunofluorescence microscopy of FAPs cultured in growth medium (GM), adipogenic induction medium (AIM) with dimethyl sulfoxide (DMSO), and AIM with CHIR99021 at concentrations ranging from 100 nM to 50  $\mu$ M. Adipocytes were stained with Oil Red O (red), myofibroblasts with  $\alpha$ -SMA (green), and nuclei with DAPI (blue). Scale bar: 100  $\mu$ m. (B) Percentage of FAPs positively stained with Oil Red O under each condition.  $n = 3$  per group. (C) Cell viability of FAPs cultured with increasing doses of CHIR99021.  $n = 4$  per group. (D) Relative mRNA expression levels of adipogenesis-related genes (PPAR- $\gamma$ , FABP4, and CEBPA) and GSK-3 after 3 days in GM, AIM with DMSO, or 3  $\mu$ M CHIR99021.  $n = 3$  per group. (E) Western blot analysis of  $\beta$ -catenin and phosphorylated GSK-3 $\beta$  (Ser9) protein levels in FAPs after 3 days in GM, AIM with DMSO, or 3  $\mu$ M CHIR99021. \*\*\* $P < .001$ .

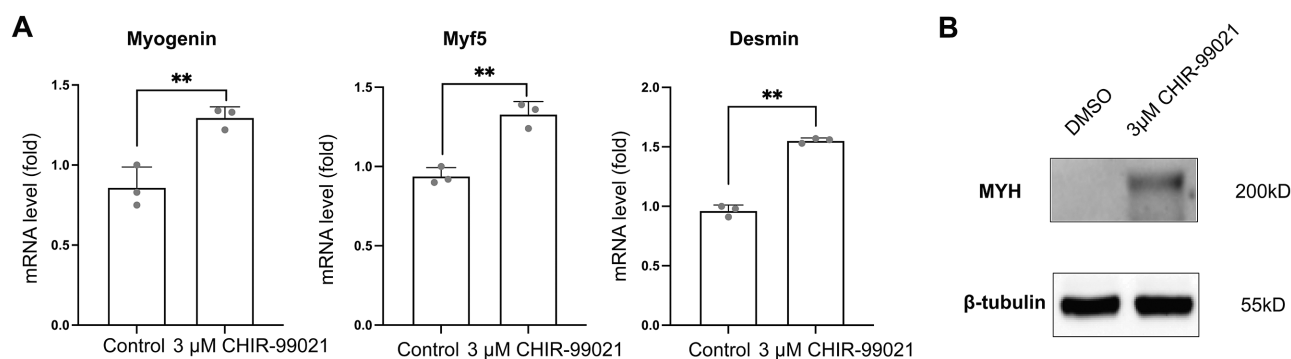


**Figure 3.** Effect of CHIR99021 on C2C12 cell differentiation. (A) Relative mRNA expression levels of myogenesis-related genes (myogenin, desmin, Myf5) after treatment with dimethyl sulfoxide (DMSO) or 3  $\mu$ M CHIR99021 for 5 days.  $n = 3$  per group. (B) Western blot analysis of myosin heavy chain levels after treatment with DMSO or 3  $\mu$ M CHIR99021 for 5 days. \*\* $P < .01$ .

significant weight differences were observed between the CHIR99021-treated and vehicle groups postoperatively, indicating low toxicity (Figure 5B). By day 26 after surgery, mice in both groups showed significant weight gain, indicating ongoing recovery and growth. No side effects or mortality were observed in the 48 mice.

Muscle weight loss was significantly decreased in the CHIR99021 group compared with the vehicle group:  $-1.32\% \pm 10.45\%$  versus  $-13.17\% \pm 12.65\%$ , respectively, at 1 week after surgery ( $P = .035$ ) and  $-39.82\% \pm 13.32\%$  versus  $-51.20\% \pm 9.12\%$ , respectively, at 4 weeks after

surgery ( $P = .048$ ) (Figure 5C). This indicated that CHIR99021 effectively prevented muscle weight loss in the supraspinatus muscle.

Gene expression analysis by RT-qPCR (Figure 5, D and E) revealed that CHIR99021 significantly reduced PPAR- $\gamma$  levels at both 1 and 4 weeks after the RCT, suggesting the suppression of fatty infiltration. Additionally, myogenesis-related genes (myogenin and Myf5) were upregulated by CHIR99021, indicating that muscle regeneration was activated by CHIR99021. Interestingly, IL-6 and IL-15 levels were elevated at 1 week after surgery with CHIR99021

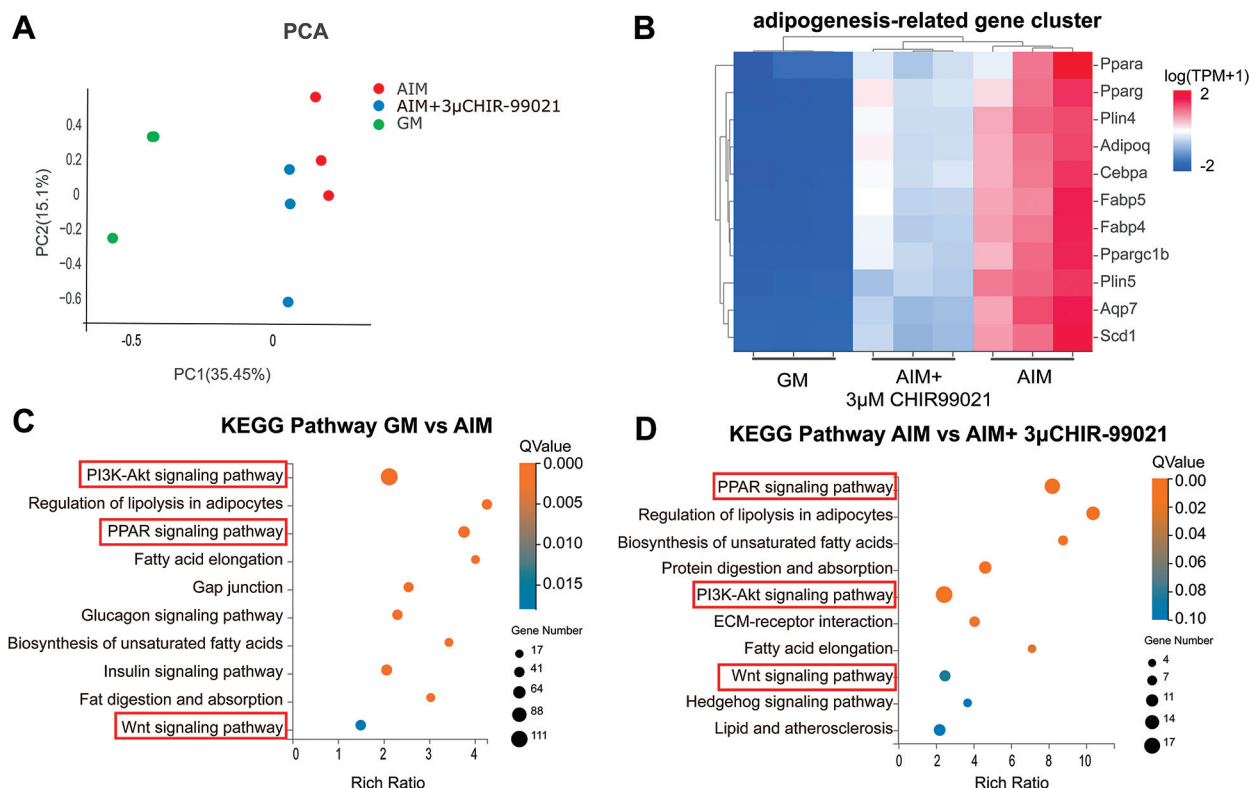


**Figure 4.** RNA sequencing analysis of fibro-adipogenic progenitors (FAPs) cultivated in different conditions. (A) Principal component analysis of FAPs in 3 conditions.  $n = 3$  per group. (B) Clustering heatmap of adipogenesis-related gene expression levels. (C) KEGG (Kyoto Encyclopedia of Genes and Genomes) pathway enrichment analysis of differentially expressed genes (DEGs) between growth medium (GM) and adipogenic induction medium (AIM). (D) KEGG pathway enrichment analysis of DEGs between AIM and AIM + 3  $\mu$ M CHIR99021.

treatment but returned to control levels by 4 weeks, implying a transient inflammatory response.

Consistent with the gene expression level, histological findings also demonstrated reduced fatty infiltration and muscle atrophy in the CHIR99021 group compared with the vehicle group at 1 and 4 weeks after surgery (Figure 6, A and B, and Figure 7B). Quantitatively, the percentage of areas stained with Oil Red O was significantly lower in the CHIR99021 group compared with the control group:  $0.44\% \pm 0.14\%$  versus  $1.44\% \pm 0.10\%$ , respectively ( $P < .01$ ) (Figure 6C). Furthermore, muscle atrophy was reduced in the CHIR99021-treated group, as the CHIR99021 group ( $2526.98 \pm 137.82 \mu\text{m}^2$ ) exhibited a significantly larger myofiber cross-sectional area at 4 weeks compared with the control group ( $1474.43 \pm 156.63 \mu\text{m}^2$ ) ( $P < .001$ ) (Figure 7C).

In addition, at 4 weeks after surgery, a significant reduction in the population of PDGFR $\alpha$ -positive FAPs was observed in the CHIR99021 group compared with the control group (Figure 7D). This suggests that CHIR99021 effectively attenuated the expansion of FAPs, which are critical contributors to fatty infiltration after RCTs. In summary, CHIR99021 demonstrated low toxicity, suppressed fatty infiltration, and enhanced myogenesis in

a mouse RCT model, emphasizing its potential as a treatment option for rotator cuff degeneration.

## DISCUSSION

Our study demonstrated that the Akt/GSK-3/ $\beta$ -catenin pathway is a crucial regulator of adipogenesis. The GSK-3 inhibitor CHIR99021 showed remarkable therapeutic effects by suppressing fat accumulation and promoting myogenesis both in vivo and in vitro.

We conducted RNA sequencing analysis on supraspinatus samples from patients with chronic RCTs to investigate the pathways involved in fatty infiltration. This approach enabled us to create a more accurate and patient-relevant transcriptomic database. A comparison of Goutallier stage 0 and stage 2 samples revealed that DEGs were enriched in the PPAR pathway, with PPAR- $\gamma$  identified as a central transcriptional modulator of adipocyte differentiation.<sup>28</sup> Additionally, the PI3K-Akt and Wnt pathways were significantly enriched, although their roles in RCTs have been rarely explored. Lin et al<sup>25</sup> reported that the Akt activator SC79 reduces the adipogenesis of mouse FAPs. Their results also demonstrated that the  $\beta$ -catenin activator



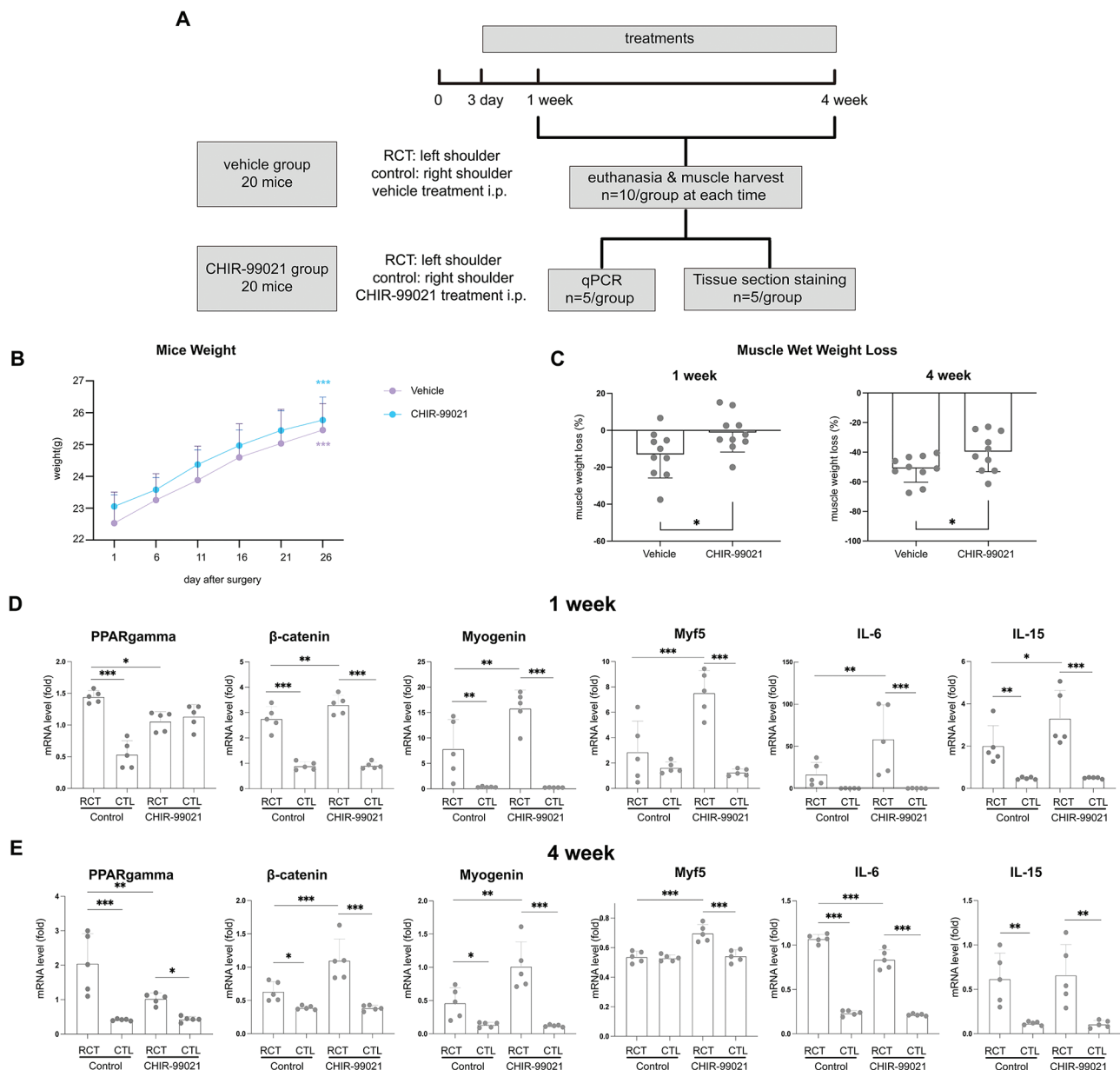


**Figure 5.** Overview of the experimental design, mouse weight and muscle weight analysis, and gene expression levels in the supraspinatus muscle. (A) Schematic diagram of the animal experiment. (B) Weight of mice after surgery. (C) Muscle wet weight loss of the supraspinatus in the 2 groups at 1 and 4 weeks after surgery. (D, E) Reverse transcription–quantitative polymerase chain reaction analysis of supraspinatus muscle tissue for adipogenic, myogenic, and inflammation-related gene expression levels at 1 and 4 weeks after surgery. \* $P < .05$ ; \*\* $P < .01$ ; \*\*\* $P < .001$ .

BML-284 could treat fatty infiltration and improve shoulder function after RCTs in mice. However, their study did not evaluate whether BML-284 could treat concomitant muscle atrophy. Our study focused on GSK-3, the upstream regulator of  $\beta$ -catenin. In vitro, our study demonstrated that the GSK-3 inhibitor CHIR99021 effectively suppressed the adipogenesis of FAPs through the Akt/GSK-3/ $\beta$ -catenin pathway, with relatively low toxicity. CHIR99021 also promoted myogenesis in C2C12 cells by increasing the expression of myogenesis-related genes. In

vivo, CHIR99021 treatment significantly reduced fatty infiltration and muscle atrophy in mice with RCTs. Reggio et al<sup>31</sup> also reported that another GSK-3 inhibitor, LY2090314, limited fatty degeneration in glycerol-injured muscles in mice. Our study provides new insight into the specific effects of CHIR99021 on the RCT model and its effect on inflammation.

After RCTs, inflammation with elevated cytokine levels peaks around day 5.<sup>33</sup> The inflammatory process after an injury has an intricate relationship with myogenesis and

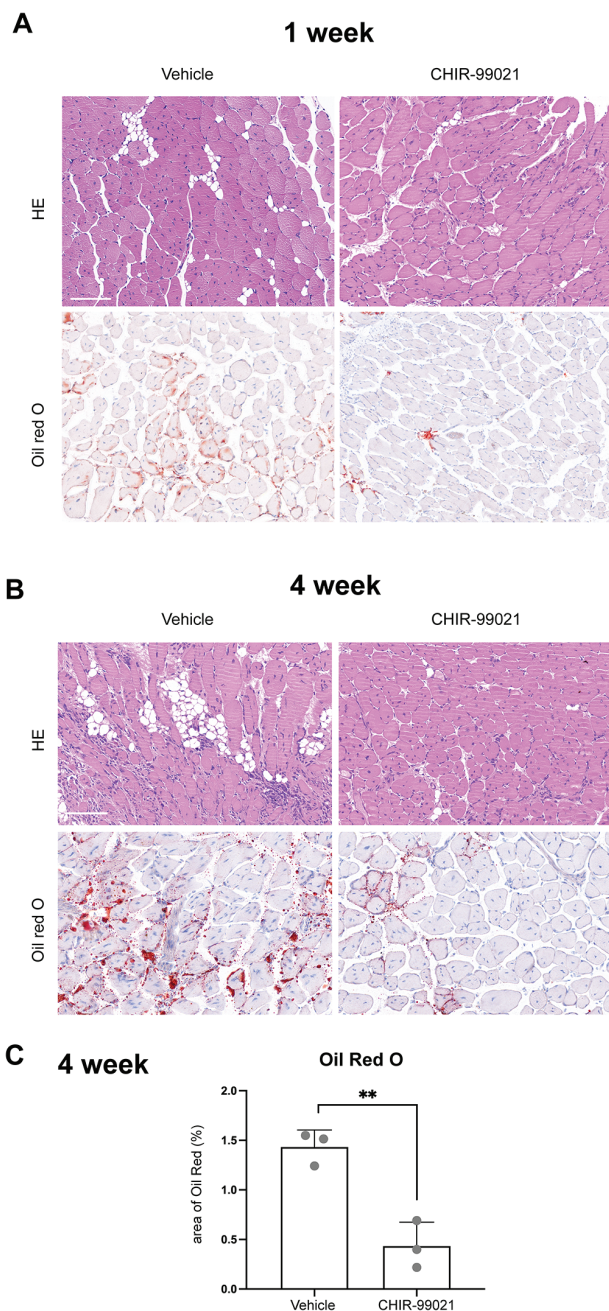


**Figure 6.** Histological analysis and quantification of fatty infiltration in the supraspinatus muscle. (A, B) Hematoxylin & eosin and Oil Red O staining of the injured supraspinatus muscle at 1 and 4 weeks after surgery. Scale bar: 100  $\mu$ m. (C) The percentage of areas stained with Oil Red O divided by the total cross-sectional area was used to determine the amount of fat accumulation at 4 weeks after surgery.  $n = 3$  per group.  $**P < .01$ .

adipogenesis in the supraspinatus muscle. Although inflammation is usually perceived negatively, it is also important for tissue repair after damage.<sup>2</sup> To elucidate the effect of RCTs and CHIR99021 on the inflammatory

environment within supraspinatus tissue, we evaluated the levels of 2 key cytokines: IL-6 and IL-15. IL-6 is a pleiotropic cytokine, exhibiting both proinflammatory and anti-inflammatory effects. According to Joe et al,<sup>12</sup> FAPs serve as an inducible source of IL-6 during muscle regeneration, supporting and promoting the differentiation of muscle stem cells. IL-6 is also one of the few myokines that are generated by skeletal muscle.<sup>29</sup> On the other hand, IL-15 is primarily proinflammatory. Kang et al<sup>13</sup> found that IL-15 administration in cardiotoxin-injured muscles significantly inhibits fatty degeneration. However, prolonged IL-15 treatment can lead to collagen and fibronectin deposition, resulting in muscle fibrosis. In our study, we observed that the mRNA expression levels of 2 cytokines, especially IL-6, were noticeably upregulated at 1 week after an RCT and then decreased by 4 weeks compared with the control (noninjured) side, indicating a transient inflammatory response aimed at injury repair. Furthermore, CHIR99021 treatment further enhanced IL-6's regenerative effects. IL-15 had a similar trend, with transient elevation of the level of IL-15 potentially contributing to the reduced formation of adipose tissue by CHIR99021 treatment. These findings suggest that CHIR99021 modulated the inflammatory response to promote muscle regeneration and mitigate fatty infiltration. However, the interplay between inflammation and muscle degeneration after an RCT requires further investigation.

GSK-3 plays a crucial role in regulating several cellular processes, including insulin signaling, glycogen synthesis, Wnt signaling, and neurotrophic factor signaling. It is considered a potential pharmaceutical target for various conditions such as diabetes mellitus, ophthalmic diseases, and cardiac hypertrophy.<sup>1</sup> According to Lee et al,<sup>20</sup> CHIR99021 was shown to inhibit fibroblast differentiation into adipocytes in Graves orbitopathy, proving the potential of CHIR99021 to suppress adipogenesis. Furthermore, CHIR99021 has been reported to inhibit fibrosis of human Tenon fibroblasts induced by TGF- $\beta$ .<sup>21</sup> TGF- $\beta$  is known to promote rotator cuff muscle fibrosis and fatty infiltration by inhibiting the apoptosis of FAPs.<sup>4</sup> Thus, CHIR99021 might also inhibit fibrosis in FAPs, potentially reducing muscle fibrosis in RCTs. Further research is warranted to explore the specific effects of CHIR99021 on TGF- $\beta$  signaling and muscle fibrosis in RCTs.

A phase 1/2 clinical trial involving FX-322 (a combination of CHIR99021 and sodium valproate) was conducted for stable sensorineural hearing loss.<sup>26</sup> Reported side effects included the minor occurrence of ear pain and headaches, with no instances of mortality or serious adverse effects observed. However, no clinical trials have yet investigated CHIR99021 for muscle diseases. Therefore, a further assessment of the potential side effects of CHIR99021 in rotator cuff degeneration is warranted for future clinical use.

## Limitations

First, because of the limited size of biopsy samples, we were unable to isolate FAPs from patients' rotator cuff tissue; thus, a further evaluation of CHIR99021 on human

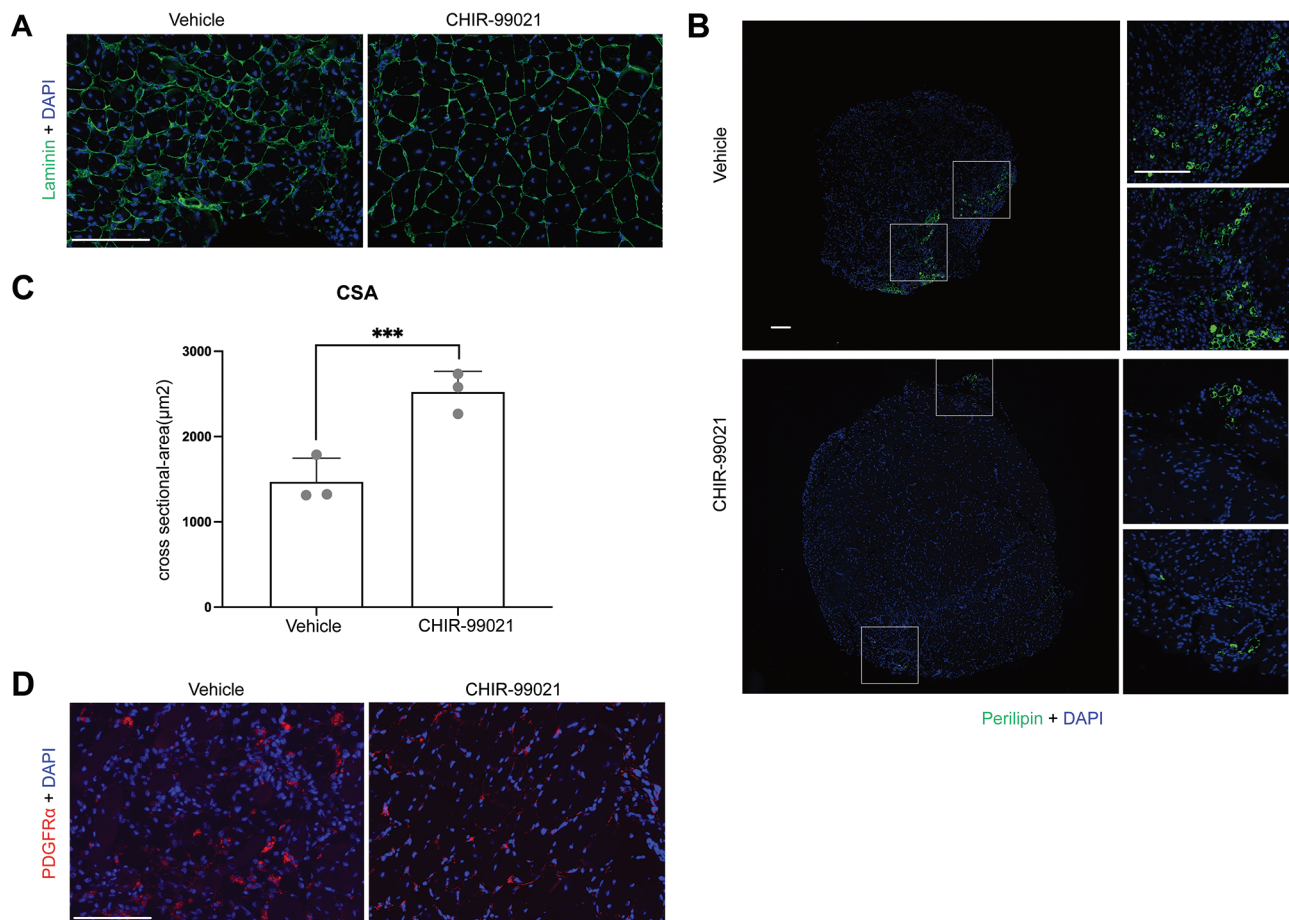


**Figure 7.** Immunofluorescence staining and cross-sectional area (CSA) analysis of the supraspinatus muscle at 4 weeks after surgery. (A) Perilipin and laminin were stained green, and cell nuclei were stained blue. Scale bar: 100  $\mu$ m. (B) Perilipin was stained green, and cell nuclei were stained blue. Scale bar: 100  $\mu$ m. (C) The CSA was calculated for the 2 groups.  $n = 3$  per group. (D) PDGFR $\alpha$  was stained red, and cell nuclei were stained blue. Scale bar: 100  $\mu$ m. \*\*\* $P$  < .001.

FAPs is needed. Second, we administered CHIR99021 via an intraperitoneal injection for its stability and ease of use. However, because RCTs are localized injuries, more targeted delivery methods may be more effective. Future research should explore localized delivery strategies for CHIR99021 to the rotator cuff muscles to minimize potential side effects. While our study evaluated the expression levels of inflammatory cytokines IL-6 and IL-15, this alone may not fully capture the complex dynamics of inflammation and its long-term effect on muscle degeneration. Additionally, our study primarily focused on histological and molecular markers of adipogenesis and myogenesis without thoroughly assessing functional outcomes such as muscle strength, range of motion, and overall shoulder function. Moreover, increasing the sample size and matching animal models more closely to human clinical conditions could further enhance the relevance and applicability of our findings. Addressing these limitations in future studies will be crucial to comprehensively understand the therapeutic potential of CHIR99021 in treating RCTs.

## CONCLUSION

Our results highlight the potential of targeting the Akt/GSK-3/ $\beta$ -catenin pathway as a therapeutic strategy for mitigating fatty infiltration and promoting muscle regeneration in RCTs. The GSK-3 inhibitor CHIR99021 effectively suppressed fat accumulation in FAPs and significantly reduced fatty infiltration and muscle atrophy in a mouse model of RCTs. These promising results indicate that GSK-3 inhibitors, such as CHIR99021, could be valuable in developing new treatment methods for rotator cuff degeneration. However, further research is essential to fully elucidate the clinical implications and optimize the therapeutic application of GSK-3 inhibitors in treating rotator cuff degeneration.

## ORCID iDs

Pu Zhang <https://orcid.org/0009-0007-9839-4552>  
Jianhao Xie <https://orcid.org/0000-0003-0456-9686>



## REFERENCES

- Beurel E, Grieco SF, Jope RS. Glycogen synthase kinase-3 (GSK3): regulation, actions, and diseases. *Pharmacol Ther.* 2015;148:114-131.
- Chazaud B. Inflammation and skeletal muscle regeneration: leave it to the macrophages! *Trends Immunol.* 2020;41(6):481-492.
- Cordani N, Pisa V, Pozzi L, Sciorati C, Clementi E. Nitric oxide controls fat deposition in dystrophic skeletal muscle by regulating fibro-adipogenic precursor differentiation. *Stem Cells.* 2014;32(4):874-885.
- Davies MR, Liu X, Lee L, et al. TGF- $\beta$  small molecule inhibitor SB431542 reduces rotator cuff muscle fibrosis and fatty infiltration by promoting fibro/adipogenic progenitor apoptosis. *PLoS One.* 2016;11(5):e0155486.
- Feeley BT, Liu M, Ma CB, et al. Human rotator cuff tears have an endogenous, inducible stem cell source capable of improving muscle quality and function after rotator cuff repair. *Am J Sports Med.* 2020;48(11):2660-2668.
- Gerber C, Meyer DC, Schneeberger AG, Hoppeler H, von Rechenberg B. Effect of tendon release and delayed repair on the structure of the muscles of the rotator cuff: an experimental study in sheep. *J Bone Joint Surg Am.* 2004;86(9):1973-1982.
- Giuliani G, Rosina M, Reggio A. Signaling pathways regulating the fate of fibro/adipogenic progenitors (FAPs) in skeletal muscle regeneration and disease. *FEBS J.* 2022;289(21):6484-6517.
- Gladstone JN, Bishop JY, Lo IK, Flatow EL. Fatty infiltration and atrophy of the rotator cuff do not improve after rotator cuff repair and correlate with poor functional outcome. *Am J Sports Med.* 2007;35(5):719-728.
- Godenèche A, Elia F, Kempf JF, et al. Fatty infiltration of stage 1 or higher significantly compromises long-term healing of supraspinatus repairs. *J Shoulder Elbow Surg.* 2017;26(10):1818-1825.
- Heredia JE, Mukundan L, Chen FM, et al. Type 2 innate signals stimulate fibro/adipogenic progenitors to facilitate muscle regeneration. *Cell.* 2013;153(2):376-388.
- Iio R, Manaka T, Takada N, et al. Parathyroid hormone inhibits fatty infiltration and muscle atrophy after rotator cuff tear by browning of fibroadipogenic progenitors in a rodent model. *Am J Sports Med.* 2023;51(12):3251-3260.
- Joe AW, Yi L, Natarajan A, et al. Muscle injury activates resident fibro/adipogenic progenitors that facilitate myogenesis. *Nat Cell Biol.* 2010;12(2):153-163.
- Kang X, Yang MY, Shi YX, et al. Interleukin-15 facilitates muscle regeneration through modulation of fibro/adipogenic progenitors. *Cell Commun Signal.* 2018;16(1):42.
- Kim C, Lee YJ, Kim SJ, et al. Subscapularis re-tears associated with preoperative advanced fatty infiltration and greater subscapularis involvement, leading to inferior functional outcomes and decreased acromiohumeral distance. *Knee Surg Sports Traumatol Arthrosc.* 2021;29(8):2624-2630.
- Kim HM, Galatz LM, Lim C, Havlioglu N, Thomopoulos S. The effect of tear size and nerve injury on rotator cuff muscle fatty degeneration in a rodent animal model. *J Shoulder Elbow Surg.* 2012;21(7):847-858.
- Kopinke D, Roberson EC, Reiter JF. Ciliary hedgehog signaling restricts injury-induced adipogenesis. *Cell.* 2017;170(2):340-351.e12.
- Kuzel BR, Grindel S, Papandrea R, Ziegler D. Fatty infiltration and rotator cuff atrophy. *J Am Acad Orthop Surg.* 2013;21(10):613-623.
- Lansdown DA, Lee S, Sam C, et al. A prospective, quantitative evaluation of fatty infiltration before and after rotator cuff repair. *Orthop J Sports Med.* 2017;5(7):2325967117718537.
- Laron D, Samagh SP, Liu X, Kim HT, Feeley BT. Muscle degeneration in rotator cuff tears. *J Shoulder Elbow Surg.* 2012;21(2):164-174.
- Lee JS, Chae MK, Kikkawa DO, Lee EJ, Yoon JS. Glycogen synthase kinase-3 $\beta$  mediates proinflammatory cytokine secretion and adipogenesis in orbital fibroblasts from patients with Graves' orbitopathy. *Invest Ophthalmol Vis Sci.* 2020;61(8):51.
- Lee SY, Chae MK, Yoon JS, Kim CY. The effect of CHIR 99021, a glycogen synthase kinase-3 $\beta$  inhibitor, on transforming growth factor  $\beta$ -induced tenon fibrosis. *Invest Ophthalmol Vis Sci.* 2021;62(15):25.
- Lee YS, Kim JY, Oh KS, Chung SW. Fatty acid-binding protein 4 regulates fatty infiltration after rotator cuff tear by hypoxia-inducible factor 1 in mice. *J Cachexia Sarcopenia Muscle.* 2017;8(5):839-850.
- Lees-Shepard JB, Yamamoto M, Biswas AA, et al. Activin-dependent signaling in fibro/adipogenic progenitors causes fibrodysplasia ossificans progressiva. *Nat Commun.* 2018;9(1):471.
- Lemos DR, Babaeijandaghi F, Low M, et al. Nilotinib reduces muscle fibrosis in chronic muscle injury by promoting TNF-mediated apoptosis of fibro/adipogenic progenitors. *Nat Med.* 2015;21(7):786-794.
- Lin X, Wang P, Wang W, et al. Suppressed Akt/GSK-3 $\beta$ / $\beta$ -catenin signaling contributes to excessive adipogenesis of fibro-adipogenic progenitors after rotator cuff tears. *Cell Death Discov.* 2023;9(1):312.
- McLean WJ, Hinton AS, Herby JTJ, et al. Improved speech intelligibility in subjects with stable sensorineural hearing loss following intratympanic dosing of FX-322 in a phase 1b study. *Otol Neurotol.* 2021;42(7):e849-e857.
- Melis B, DeFranco MJ, Chuinard C, Walch G. Natural history of fatty infiltration and atrophy of the supraspinatus muscle in rotator cuff tears. *Clin Orthop Relat Res.* 2010;468(6):1498-1505.
- Mota de Sá P, Richard AJ, Hang H, Stephens JM. Transcriptional regulation of adipogenesis. *Compr Physiol.* 2017;7(2):635-674.
- Muñoz-Cánoves P, Scheele C, Pedersen BK, Serrano AL. Interleukin-6 myokine signaling in skeletal muscle: a double-edged sword? *FEBS J.* 2013;280(17):4131-4148.
- Naujok O, Lentjes J, Diekmann U, Davenport C, Lenzen S. Cytotoxicity and activation of the Wnt/ $\beta$ -catenin pathway in mouse embryonic stem cells treated with four GSK3 inhibitors. *BMC Res Notes.* 2014;7:273.
- Reggio A, Rosina M, Palma A, et al. Adipogenesis of skeletal muscle fibro/adipogenic progenitors is affected by the WNT5a/GSK3/ $\beta$ -catenin axis. *Cell Death Differ.* 2020;27(10):2921-2941.
- Shirasawa H, Matsumura N, Yoda M, et al. Retinoic acid receptor agonists suppress muscle fatty infiltration in mice. *Am J Sports Med.* 2021;49(2):332-339.
- Stengaard K, Hejbøl EK, Jensen PT, et al. Early-stage inflammation changes in supraspinatus muscle after rotator cuff tear. *J Shoulder Elbow Surg.* 2022;31(7):1344-1356.
- Uezumi A, Fukada S, Yamamoto N, Takeda S, Tsuchida K. Mesenchymal progenitors distinct from satellite cells contribute to ectopic fat cell formation in skeletal muscle. *Nat Cell Biol.* 2010;12(2):143-152.
- Uezumi A, Ito T, Morikawa D, et al. Fibrosis and adipogenesis originate from a common mesenchymal progenitor in skeletal muscle. *J Cell Sci.* 2011;124(Pt 21):3654-3664.
- Wang Z, Liu X, Davies MR, et al. A mouse model of delayed rotator cuff repair results in persistent muscle atrophy and fatty infiltration. *Am J Sports Med.* 2018;46(12):2981-2989.
- Yang Z, Zhang M, Liu T, et al. Does the fatty infiltration influence the re-tear rate and functional outcome after rotator cuff repair? A systematic review and meta-analysis. *Indian J Orthop.* 2023;57(2):227-237.
- Yoon JP, Park SJ, Kim DH, Chung SW. Metformin increases the expression of proinflammatory cytokines and inhibits supraspinatus fatty infiltration. *J Orthop Surg Res.* 2023;18(1):674.
- Zhao L, Son JS, Wang B, et al. Retinoic acid signalling in fibro/adipogenic progenitors robustly enhances muscle regeneration. *EBioMedicine.* 2020;60:103020.
- Zhou H, Lin X, Feng S, et al. Metformin mitigates adipogenesis of fibro-adipogenic progenitors after rotator cuff tears via activating mTOR/ULK1-mediated autophagy. *Am J Physiol Cell Physiol.* 2024;326(6):C1590-C1603.